Glymphatic Function and Ventricular Volumetry in Radiosurgery Patients

Meng-Hsin Lin[1] D12458003@ntu.edu.tw
Chao-Ya Yang[2] vivianyang03@ntuh.gov.tw
Chun-Chih Liao[3] d95548001@ntu.edu.tw
Kuo-Wei Chen[2] kwchen@ntu.edu.tw
Furen Xiao[1,2] fxiao@ntu.edu.tw

[1] *Institute of Medical Device and Imaging, National Taiwan University, College of Medicine, Taipei 100, Taiwan*
[2] *Division of Neurosurgery, National Taiwan University Hospital, Taipei 100, Taiwan*
[3] *Department of Neurosurgery, Taipei Hospital, Ministry of Health and Welfare, New Taipei City 242, Taiwan*

Editors: Under Review for MIDL 2026

Abstract

Purpose This study aimed to determine whether imaging biomarkers—specifically the ALPS index, cerebrospinal fluid (CSF) volume, and lateral ventricle (LV) volume—can serve as reliable predictors of brain aging and the tendency toward hydrocephalus, characterized by ventricular dilatation. We evaluated their individual and combined predictive power for age-related changes and early ventricular enlargement, offering a non-invasive imaging approach for clinical assessment.

Materials and Methods A total of 707 subjects who underwent radiosurgery for brain tumors between 2022 and 2024 were included (male-to-female ratio: 1:1.7; mean age 61 ± 13 years). MRI datasets included diffusion tensor imaging (DTI) and high-resolution T1-weighted scans. The ALPS index was derived to quantify glymphatic pathway efficiency, while CSF and lateral ventricle volumes were automatically extracted using SynthSeg. Statistical analyses employed linear regression to assess the relationship between these imaging markers and chronological age. Combined models were used to evaluate potential additive effects among parameters. The same setup is applied to predicting lateral ventricle volume.

Results All three imaging parameters—ALPS index, CSF volume, and total lateral ventricle volume—showed significant correlations with age ($r = 0.363$–0.424, $p < 0.001$). Larger CSF and ventricular volumes corresponded to advancing age, while a lower ALPS index indicated reduced glymphatic function. Each parameter individually provided moderate predictive strength, but combining them yielded higher consistency and precision in estimating age ($r = 0.499$) and identifying subjects showing early ventricular enlargement.

Similarly, ALPS index, CSF volume, and age each contributed meaningfully to predicting lateral ventricle volume. Individually, age ($r = 0.396$), CSF ($r = 0.460$), and ALPS index ($r = –0.566$) showed moderate correlations with ventricular enlargement. A combined regression model achieved the strongest performance ($r = 0.644$), with ALPS index emerging as the most influential predictor. These results indicate that integrating glymphatic function with structural CSF metrics provides a more stable and biologically coherent estimate of ventricular volume than any single parameter alone.

Conclusion The ALPS index, CSF volume, and lateral ventricle volume each reflect distinct yet interrelated facets of brain aging. Their integration enhances the prediction of age-related changes and the tendency toward hydrocephalus, suggesting that structural expansion and glymphatic decline are parallel hallmarks of neuroaging. These multimodal biomarkers hold promise for early, non-invasive evaluation of brain fluid and structural dynamics.

Keywords: Glymphatic system, ALPS index, CSF volume, Lateral ventricle volume, Brain aging, Neuroaging, Hydrocephalus

1. Introduction

Approximately 80% of the human brain is composed of water, which continuously shifts between various regions and cell types during both physiological and pathophysiological processes (MacAulay, 2021). Water is essential for maintaining physiological and metabolic balance. Cerebrospinal fluid (CSF) is continuously produced by the choroid plexus and circulates in the ventricular system as well as subarachnoid space. CSF buildup may arise from obstructed flow, impaired absorption, or excess production, disrupting normal intracranial homeostasis. It is associated with neurodegenerative diseases and progressive structural changes in the brain. The lateral ventricles (LV), as the largest CSF-containing cavities, are often the earliest and most visibly affected structures on neuroimaging. Chronic ventricular expansion can compromise periventricular white matter and disturb cerebral perfusion, contributing to functional deterioration. This accumulation typically causes ventricular dilatation, most notably in the lateral ventricles, resulting in increased intracranial pressure and potential brain tissue compression (Ziegelitz et al., 2015). Ventricular dilatation can compress the cerebral microvasculature, reducing cerebral perfusion (hypoperfusion) and diminishing perivascular space volume, thereby impairing glia-lymphatic (glymphatic) clearance efficiency (Chen et al., 2024).

CSF influx into brain tissue occurs along the perivascular (around blood vessels) pathway. Interstitial solute movement occurs through diffusion and advection; the latter is most rapid along intraparenchymal perivascular spaces and white matter tracts (Bohr et al., 2022). Glymphatic MRI offers noninvasive insights into metabolic and clearance function. Recent studies have demonstrated that the glymphatic system plays a crucial role in clearing interstitial macromolecules and metabolic waste products from the central nervous system, including tau proteins and amyloid beta. Consequently, dysfunction of this system may contribute to the pathogenesis of neurodegenerative diseases (Ringstad et al., 2017). There is growing interest in understanding how increased intracranial water content affects glymphatic drainage and, in turn, influences therapeutic outcomes.

Glymphatic magnetic resonance imaging (MRI) has emerged as a promising tool for evaluating cerebral metabolic function in vivo, with potential to enhance visualization of the perivascular space and provide new insights into human brain waste clearance dynamics (Ringstad et al., 2017). Diffusion Tensor Imaging–Analysis along the Perivascular Space (DTI-ALPS) measures anisotropic diffusion in the brain's white matter (Taoka et al., 2017). It specifically compares water diffusion along directions parallel vs. perpendicular to the perivascular spaces. DTI-ALPS is chosen because it offers a practical, non-invasive, and quantifiable way to assess glymphatic function—making it especially valuable in diseases like hydrocephalus where CSF clearance is impaired.

Several reports show negative correlations between age and ALPS-index, e.g., in subjects with Parkinson's Disease or essential tremor, and healthy elderly subjects (Taoka et al., 2024). CSF buildup is associated with progressive structural changes in the brain, while ventricular enlargement is associated with neurocognitive decline, gait disturbance, and urinary incontinence—the classical clinical triad of normal pressure hydrocephalus (NPH). The normalized lateral ventricle volume was found to be strongly and significantly correlated with the regional Parenchymal Cerebrospinal Fluid Fraction (CSFF) measurements in brain regions (cerebral white matter, cortex, and subcortical deep gray matter) with correlation coefficients (ρ) around 0.62 to 0.66 ($p < 0.001$ for all) (Zhou et al., 2023). This suggests that as the macroscopic CSF space (ventricles) enlarges with age, the microscopic CSF space within the brain tissue (CSFF) also enlarges, indicating that these two forms of CSF-filled space are related in the aging process. However, currently there is yet to have integrative validation across all three biomarkers (ALPS index, CSF volume, and ventricular volume) in large clinical population studies.

2. Objective/ Purpose

This study aimed to determine whether imaging biomarkers—specifically the ALPS index, CSF space volume, and lateral ventricle volume—can serve as reliable predictors of brain aging and the tendency toward hydrocephalus. We evaluated their individual and combined predictive power for age-related changes and early ventricular enlargement, offering a non-invasive imaging approach for clinical assessment.

This study aims to determine if ALPS index, CSF space volume, and lateral ventricle volume can individually and combined predict brain age using a regression model.

Another aim is to determine if ALPS index, CSF space volume, and age can individually and combined predict lateral ventricle volume using a regression model.

3. Methods

3.1. Study design

This study is a retrospective observational cohort study analyzing brain MRI data obtained from the electronic medical records of National Taiwan University Hospital (NTUH) between 2022 and 2024.

The data were drawn from the electronic medical records and PACS database of NTUH. All patients who underwent cyberknife surgery between 2022 and 2024 were considered for analysis. MRI were taken prior to surgeries, and MRI datasets include diffusion tensor imaging (DTI) and high-resolution T1-weighted scans.

3.2. Study population

The study population consists of adult patients (20–96 years old) who received brain MRI at NTUH. A total of 707 subjects who underwent radiosurgery for various brain neurological and neurosurgical pathologies between 2022 and 2024 were included, with male-to-female ratio at 1:1.7, and mean age 61 $\pm$ 13 years.

Patients who underwent cyberknife surgeries at NTUH were mainly diagnosed as Benign Neoplasm of Cerebral Meninges (brain tumors), Congenital Anomalies of Cerebrovascular System such as Arteriovenous Malformation (AVM) and Arteriovenous Fistula (AVF), and Trigeminal Neuralgia.

3.3. Inclusion and exclusion criteria

Inclusion Criteria:

1. Patients undergone CyberKnife surgery within 2022 through 2024;
2. Age $\geq$ 20 years;

Exclusion Criteria:

1. Ineligibility for surgical procedures;
2. Comorbidities likely to limit life expectancy to less than two years (e.g., advanced malignancy, heart failure, or end-stage liver disease);
3. Contraindications for cerebral MRI, including severe claustrophobia or presence of non-MRI-compatible pacemakers.

3.4. MRI setting

The subjects underwent brain MRIs on a Siemens MAGNETOM Aera 1.5T scanner (Siemens Healthineers, Erlangen, Germany) using a product 64-channel receiver coil (the maximum number of independent receiver channels that can be used simultaneously).

The brain imaging protocol consisted of:

- 3D T1-weighted (T1W) MPRAGE (Magnetization-Prepared Rapid Acquisition Gradient Echo) for high-resolution anatomical structure (`3D_T1_MPRAGE_MPR_Tra`).
- DTI (Diffusion Tensor Imaging) sequence (`ax_DTI_12dir`).
- Axial 3D T1-weighted with Magnetization Transfer (MT) and Fat Saturation (FS), with contrast administration (`AX_3D_f13d_mt_FS_MPR_Tra`).
- T2-weighted FLAIR sequence (`TRU_ax_F2_FLAIR_3mm`).

3.5. Image post-processing: ALPS index

The glymphatic system was non-invasively evaluated using Diffusion Tensor Image Analysis along the Perivascular Space (DTI-ALPS), a technique introduced by Professor Toshiaki Taoka (Taoka et al., 2017). The ALPS index serves as a quantitative radiological biomarker that reflects the activity of the glymphatic system, primarily along the medullary veins. The MRI protocol for this assessment adhered strictly to the methodology described by Taoka et al. (2017), utilizing specific DTI images acquired during the scanning session. The ALPS index was then calculated using the open-source software library alps (Barišano, G.) by methods detailed in Liu et al. (2024). This calculation involves assessing the primary

differences in diffusion coefficients: comparing the diffusion coefficients along the x-axis in projection and association fibers (D_{xxproj} and $D_{xxassoc}$) against the diffusion coefficients perpendicular to the x-axis but not aligned with major fiber tracts (D_{yyproj} and $D_{zzassoc}$). This method allows for the estimation of the presence and activity of the perivascular space as a measure of glymphatic function.

3.6. Image post-processing: Segmentation

For quantitative volumetric analysis of brain structures, all 3D T1-weighted MR images of these 707 subjects were processed using SynthSeg, a robust, publicly available deep learning-based segmentation tool (Billot et al., 2023). This automated pipeline was utilized to segment the images and calculate the volume of over 100 distinct neuroanatomical structures. Among them are CSF volumes as well as lateral ventricle volumes as the sum of left and right lateral ventricles.

3.7. Statistical analysis

Data were analyzed using linear regression to determine the predictors of the respective variables.

Initially, brain age was predicted for individual subjects from NTUH CyberKnife data (N=707) using simple linear regression.

- Dependent variable (the outcome being predicted): brain age.
- Independent variables (the predictors): ALPS index, CSF volume, and lateral ventricle volume.

Then, based on the predicted age for each input MRI feature, we examined the discrepancy between these predicted ages and the actual biological age.

Likewise, lateral ventricle volume was predicted for individual subjects from NTUH CyberKnife data (N=707) using simple linear regression.

- Dependent variable (the outcome being predicted): lateral ventricle volume.
- Independent variables (the predictors): ALPS index, CSF volume, and age.

Then, based on the predicted lateral ventricle volume for each input MRI feature, we examined the discrepancy between these predicted lateral ventricle volumes and the actual volume.

Subsequently, a multiple linear regression was applied to determine the combined effect of all predictor variables on the outcome and to assess the independent contribution of each predictor. In other words, ALPS index, CSF volume, and lateral ventricle volume are combined to predict brain age, while ALPS index, CSF volume, and age are combined to predict lateral ventricle volume.

4. Results

4.1. Baseline data

Table 1 shows the means, standard deviations, and ranges of the predictor variables (CSF volume, Lateral Ventricle Volume, DTI-ALPS index, and Age).

Table 1: Descriptive characteristics of volumetric measurements

Key Variables	**Mean ± SD**	**Median**	**Range**
CSF volume (c.c.)	327.95 ± 50.2	319.11	220.45 ∼ 533.59
Lateral Ventricle volume (c.c.)	29.96 ± 17.6	24.91	5.80 ∼ 117.82
DTI-ALPS index (unitless)	1.36 ± 0.21	1.36	0.39 ∼ 2.06
Age (years old)	61 ± 13	62	21 ∼ 96

4.2. Statistical regression analysis

Overall Model Fit: The p-values are extremely small ($p < 0.001$), indicating that the models are highly statistically significant, well predicting the outcome for linear regression.

Table 2: Correlation of Age with Following Variables, in the order of p-value.

Key Variables	**Equation**	**R**	**p-value**
DTI-ALPS index	y = -0.0069x + 1.7815	-0.4243	$p < 0.001$
Lateral Ventricle volume	y = 531.89x - 2578.2	0.3964	$p < 0.001$
CSF volume	y = 1387.1x + 243088	0.3630	$p < 0.001$

Table 3: Correlation of Lateral Ventricle Volume, in the order of p-values.

Key Variables	**Equation**	**R**	**p-value**
DTI-ALPS index	y = -7E-06x + 1.5663	-0.5659	$p < 0.001$
CSF volume	y = 1.3084x + 288747	0.4595	$p < 0.001$
Age	y = 0.0003x + 52.326	0.3964	$p < 0.001$

Table 4: Multiple Linear Regression of Predicting Age and Lateral Ventricle Volume.

Outcome Variable	**Equation**	**R**	**p-value**
Predicting Age	Age = 63.3027 + 0.00010954*LV + 0.00005384*CSF − 16.93325*ALPS	0.4990	$p < 0.001$
Predicting Lateral Ventricle volume	Total Lateral Ventricle = 36710.61 + 0.097687*CSF -35383.2*ALPS + 153.843·Age	0.6437	$p < 0.001$

4.2.1. Predict Brain Age

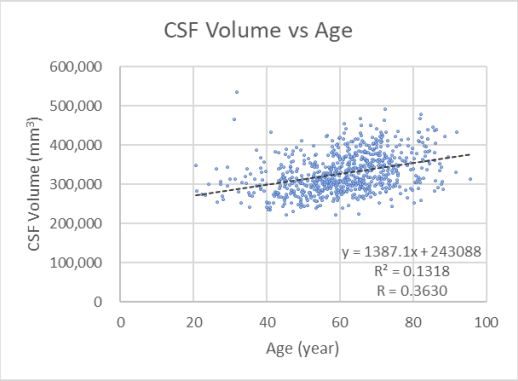

Figure 1: Correlation of Age with Cerebral Spinal Fluid (CSF) volume

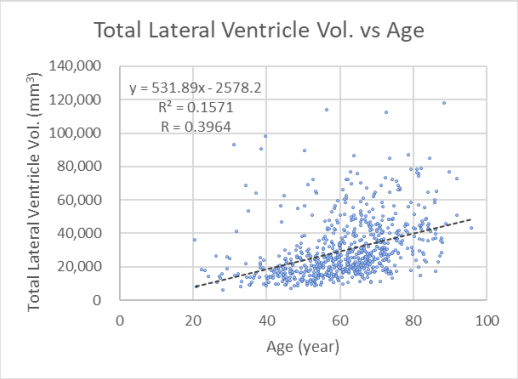

Figure 2: Correlation of Age with Lateral Ventricle volume

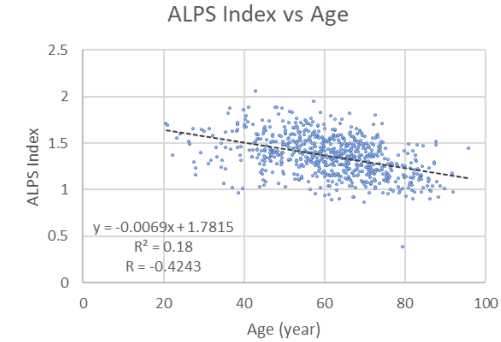

Figure 3: Correlation of Age with ALPS index

4.2.2. Predict Lateral Ventricle Volume

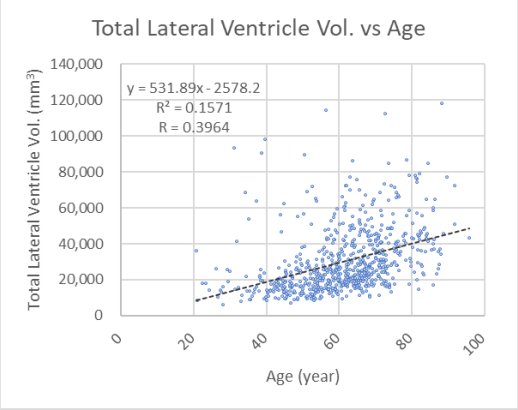

Figure 4: Correlation of Lateral Ventricle volume with Age

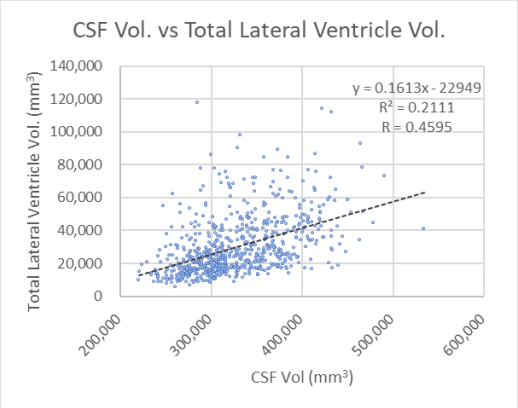

Figure 5: Correlation of Lateral Ventricle volume with CSF volume

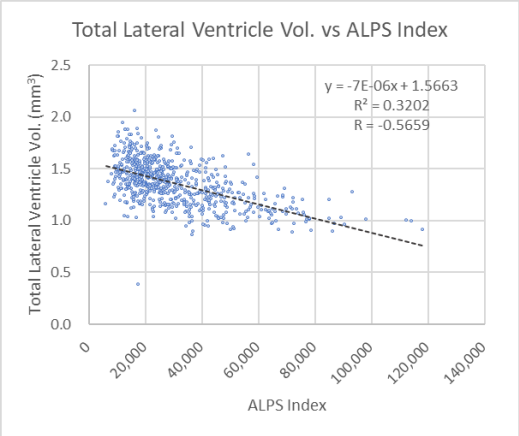

Figure 6: Correlation of Lateral Ventricle volume with ALPS index

4.3. High-Residual Cases

For predicting brain age or lateral ventricle volumes using multiple variable regression models, the correlation is somewhat strong, but there are still points straying from the correlation lines. The points straying farthest from the correlation lines are shown below.

4.3.1. Predicted age larger than actual physical age (worse than actual)

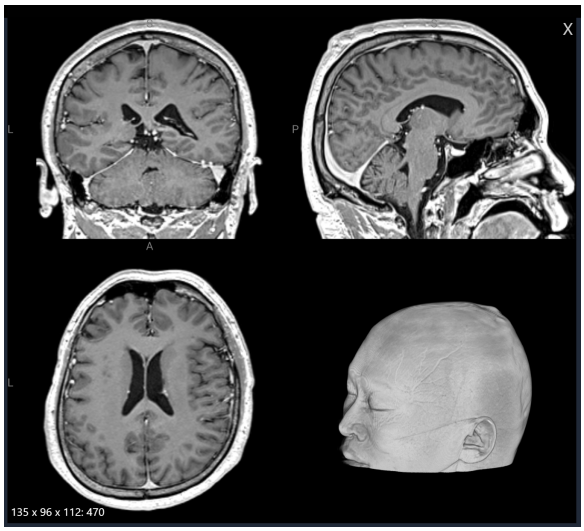

Figure 7: This patient had a seizure. Diagnosed to have Arteriovenous Fistula located at right posterior insula. Age 32, predicted to be 74, with large CSF value 533.6 cc. as well as large lateral ventricle volume 41.1 cc.

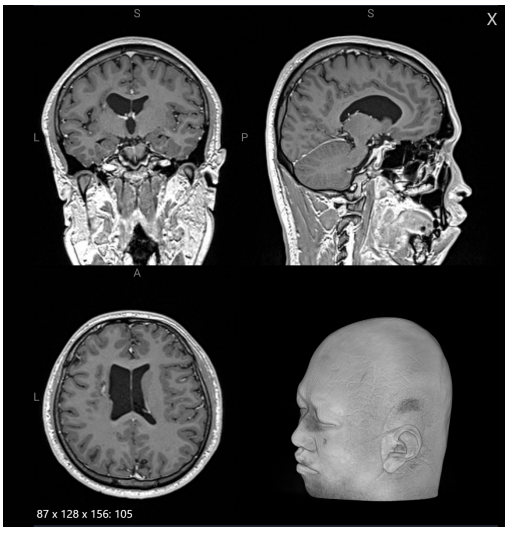

Figure 8: This patient has Congenital Anomalies of Cerebrovascular System with right frontal AVM. Age 21 only, predicted to be 57. Lateral ventricle volume is 36.2 cc, 4.3 times that of predicted.

4.3.2. Predicted age smaller than actual physical age (better than actual)

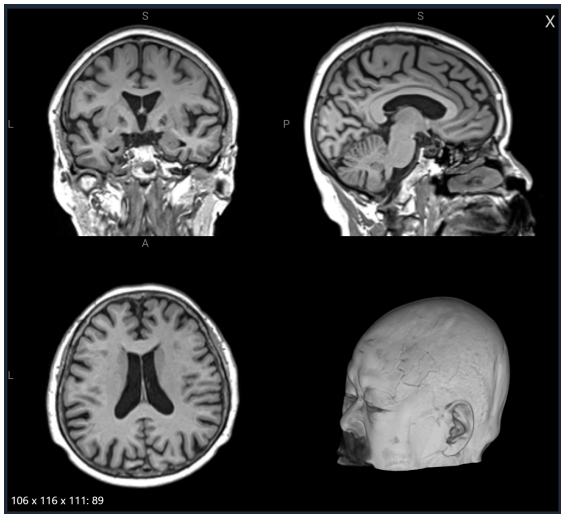

Figure 9: This patient has Secondary Malignant Neoplasm of Brain and Spinal Cord, and Lung cancer with brain metastases. Age 88, predicted to be 57. ALPS index as high as 1.52, predicted to be 1.18. The lateral ventricle volume (28.1 cc) is also 64% of predicted.

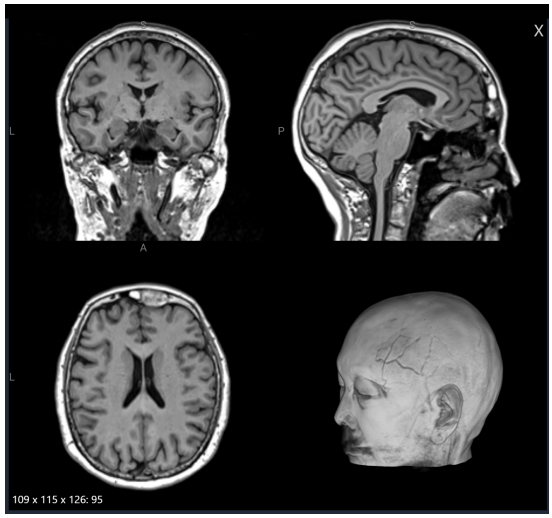

Figure 10: This patient has Secondary Malignant Neoplasm Of Brain And Spinal C and Malignant neoplasm of unspecified part of left bronchus or lung. Age 75, predicted to be 49. ALPS value of 1.71 while predicted to be only 1.27.

4.3.3. Predicted values larger than actual Lateral Ventricle volume (actual is better)

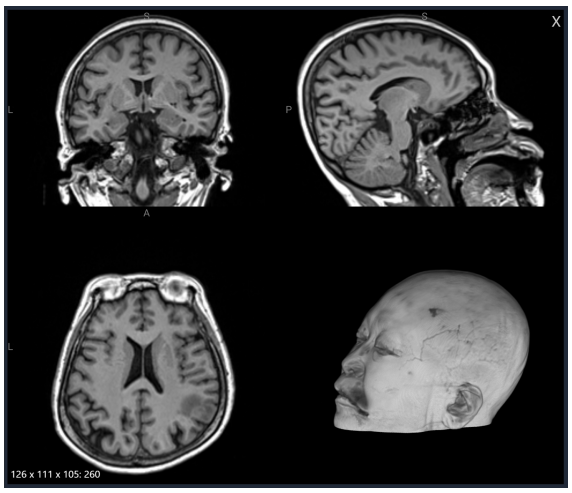

Figure 11: This patient has Secondary Malignant Neoplasm of Brain and Spinal Cord. LV of 13.6 cc, better than predicted 39.6 cc. At age 66, ALPS number is 1.04, worse than predicted 1.47; however, the subject is actually younger than predicted age of 56.

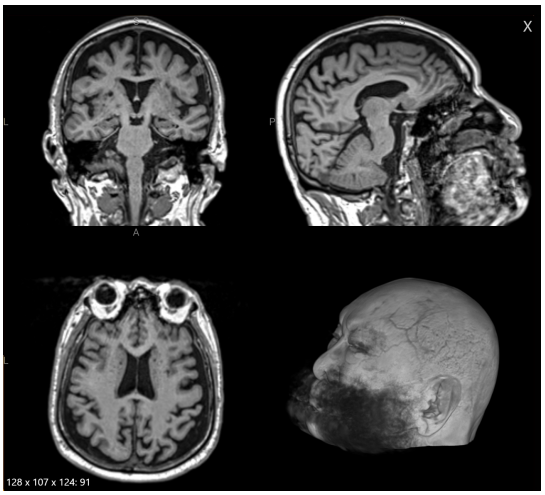

Figure 12: This patient has Secondary Malignant Neoplasm of Brain and Spinal Cord, Lung cancer with brain metastases. LV 22.5 cc, better than predicted 54.4 cc. At age 84, large CSF leads to larger predicted LV. ALPS is only 1.10 while predicted to be 1.41. However, the predicted age is 59, much younger than actual.

4.3.4. Predicted values smaller than actual Lateral Ventricle volume (actual is worse)

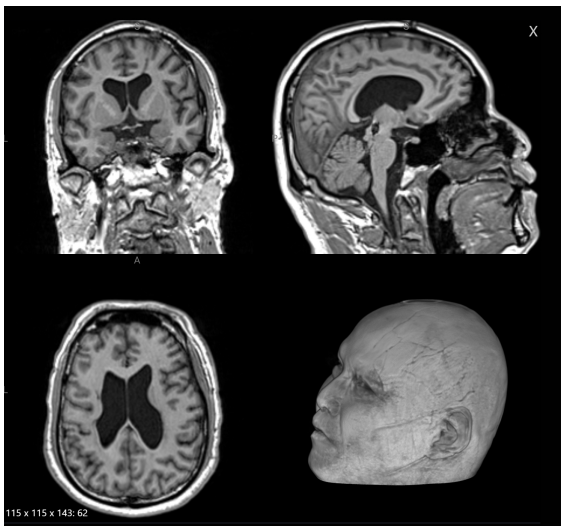

Figure 13: This patient has Congenital Anomalies of Cerebrovascular System, and Right midbrain cavernoma. Also with shunt. LV 97.8 cc but predicted to be 45.8 only. Although CSF is 331.7 cc, smaller than predicted 416.8 cc. The age, 40, is predicted to be 82.

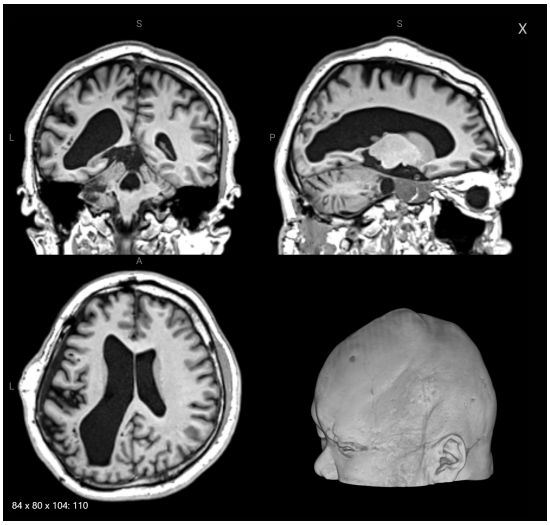

Figure 14: This patient has Benign Neoplasm of Cranial Nerves. LV 92.9 c.c but predicted to be 38.5 cc only. Although the ALPS index is 1.28, much better than predicted 0.92. However, at age 31, the subject is predicted to be 80 years old.

5. Discussion

5.1. Summary of Key Findings:

5.1.1. Single variable prediction

The correlation of each of the three variables used for predicting brain age is moderately strong. The correlation, from relatively strongest to weakest, is ALPS, followed by Total Lateral Ventricle, with Cerebral Spinal Fluid being the weakest. Although ALPS is with the strongest correlation index, it is negatively correlated, indicating that the larger the ALPS index is, the smaller the brain age it predicts. The three correlation values are -0.4243, 0.3964, and 0.3630 respectively.

In contrast, if using the age, CSF, and ALPS to predict the total lateral ventricle volume, the correlations seem stronger: Using age to predict, the correlation is 0.3964; CSF to predict, 0.4595; ALPS index to predict, -0.5659.

ALPS index gives the strongest correlation whether to predict brain age or to predict lateral ventricle volume.

5.1.2. Multivariable prediction

Using three variables combined to predict brain age, we get the following equation:

$$Age = 63.3027 + 0.00010954 * LV + 0.00005384 * CSF – 16.93325 * ALPS$$

where ALPS is the strongest contributor in this model with R = 0.4990.

Using three variables combined to predict total lateral ventricle volume, we get

$$TotalLateralVentricle = 36710.61 + 0.097687 * CSF - 35383.2 * ALPS + 153.843 * Age$$

where ALPS is still the strongest contributor in this model with R = 0.6437.

5.2. Interpretation and Comparison:

The cluster of extreme values was traced back to specific patient groups.

5.2.1. Predicted age larger than actual physical age (worse than actual)

The majority of the pathologies involve arteriovenous shunting, including both congenital AVMs in the cerebellum and frontal lobe, and acquired AVFs, one of which is complicated by epilepsy. The remaining case is a benign neoplasm of the cranial nerves. Overall, the cases represent common, complex vascular and tumor neurosurgical conditions.

Both AVMs and AVFs can lead to complications such as hemorrhage, high venous pressure, and epilepsy. These neurological issues of blood "stealing" from brain tissue or causing pressure buildup are known to create a chronic state of hemodynamic stress on the surrounding brain tissue, which can accelerate imaging features typically associated with aging.

The presence of AVMs and AVFs can lead to cerebral hypoperfusion (reduced blood flow) in adjacent brain regions, chronic low-grade inflammation, or microvascular damage due to the high-flow shunt. These processes are known to contribute to tissue changes, like volume loss and increased perivascular space visibility. The chronic presence of an AVM or AVF, even if asymptomatic, may lead to structural degeneration that is quantified by the regression model as an "older" brain age.

5.2.2. Predicted age smaller than actual physical age (better than actual)

This case collection highlights some instances of secondary malignant neoplasms of the brain and spinal cord, all originating as metastatic lung cancer. This heavy representation of metastatic disease emphasizes the high morbidity associated with systemic malignancy and suggests a tertiary referral pattern. Conversely, the remaining cases involve primary, non-cancerous issues: a benign meningioma (Right frontal) and an acquired AVF involving the sigmoid sinus.

The brain structure appears healthier, or less degenerated, than expected for their years. Despite the presence of focal or contained pathologies (metastasis, meningioma, AVF), these specific lesions are not the primary drivers of global structural deterioration. With high ALPS index, small ratio of predicted LV or CSF, the patient's underlying biological brain aging process, as measured by the chosen quantitative imaging biomarkers, is proceeding slower than average.

5.2.3. Predicted values larger than actual LV (actual is better)

The analysis of this neurosurgical cohort, which includes AVFs, Congenital AVMs, and Benign Neoplasms of the Cranial Nerves and Cerebral Meninges, revealed a consistent trend of structural preservation. Across all subjects, the Actual Lateral Ventricle volume was significantly smaller than the volume predicted by the aging model.

This outcome suggests that the patients' brain structure is more preserved, or "younger", than expected for their chronological age. This finding implies that the listed pathologies are focal and localized, and are not the primary drivers of diffuse, global atrophy typically associated with an "older" brain in these prediction models. The LV volumes indicate that the macroscopic atrophy feature of aging is highly under-expressed in this group.

Despite the remarkable preservation of macroscopic structure (small LV volumes), a discrepancy was noted in the ALPS index, a measure of microscopic perivascular space (glymphatic) activity. The ALPS index was consistently worse (lower) than the predicted value, indicating compromised glymphatic function. This suggests a decoupling between the structurally preserved macro-CSF space (LV volume) and the failing microscopic clearance system (glymphatic function), a trend that warrants further investigation to understand the specific impact of these pathologies on CSF dynamics.

5.2.4. Predicted values smaller than actual LV (actual is worse)

This cohort, comprising patients with Congenital Vascular Anomalies (AVM/ Cavernoma), Benign Neoplasms, and Secondary Malignant Neoplasms, exhibits a striking and uniform trend of accelerated structural aging. All subjects display a Lateral Ventricle volume much larger than predicted (90.4 cc–117.8 cc actual vs. 38.5 cc–45.8 cc predicted), which suggests significant macroscopic atrophy leading to a greatly enlarged LV.

This severe structural deterioration is reflected in the predicted age, with the majority of subjects being predicted as decades older than their chronological age (e.g., age 31 predicted as 80, age 40 predicted as 82). Despite this severe LV enlargement, some subjects showed an ALPS index better (higher) than predicted, suggesting that the microscopic perivascular space activity may be disproportionately preserved or even upregulated relative to the severe ventricular dilation and apparent age.

The highly elevated LV volumes and older predicted ages across these diverse focal pathologies suggest that the lesions, including vascular malformations, tumors, and shunts, may induce chronic, diffuse damage or long-standing altered CSF hydrodynamics that accelerate global brain atrophy. This contrasts sharply with cohorts where LV volume is preserved.

6. Conclusion

The analysis across different neurosurgical cohorts reveals a profound influence of pathology type on the structural aging phenotype. Cases where the Predicted Age is smaller than the Actual Age show remarkably preserved macroscopic structure (Actual LV $<$ Predicted LV), suggesting their focal pathologies (meningiomas, early metastases, etc.) are not the primary drivers of global atrophy. This preservation highlights that the patient's underlying biological aging process, as measured by macro-structural biomarkers, is pro-

ceeding slower than average. In contrast, cohorts where the Predicted Age is much larger than the Actual Age display accelerated structural deterioration (Actual LV > Predicted LV). These pathologies, typically severe vascular malformations (AVMs/AVFs) or obstructive lesions, introduce a powerful confounding factor that mimics or accelerates age-related atrophy, often through chronic CSF alterations or hemodynamic stress. Crucially, the inconsistent ALPS index results across both trends underscore a decoupling between macroscopic preservation and microscopic glymphatic activity, validating the model's clinical utility in detecting underlying pathological processes that drive brain aging beyond the typical rate.

References

Benjamin Billot, You Colin, Magdamo Cheng, Sudeshna Das, and Juan Eugenio Iglesias. Robust machine learning segmentation for large-scale analysis of heterogeneous clinical brain MRI datasets. *Proceedings of the National Academy of Sciences (PNAS)*, 120(9): 1–10, 2023. doi: 10.1073/pnas.2216399120.

Tomas Bohr, Poul G. Hjorth, Stine C. Holst, Silvie Hrabětová, Vesa Kiviniemi, Tom Lilius, Iben Lundgaard, Kent-Andre Mardal, Erik A. Martens, Yoshinori Mori, U. Valentin Nägerl, Charles Nicholson, Allen Tannenbaum, James H. Thomas, Jonathan Tithof, Helene Benveniste, Jeffrey J. Iliff, Douglas H. Kelley, and Maiken Nedergaard. The glymphatic system: Current understanding and modeling. *iScience*, 25(9):104987, September 2022. doi: 10.1016/j.isci.2022.104987.

Kuo-Wei Chen, Yen-Ru Chen, Li-Ying Yang, Yi-Wen Cheng, Sheng-Chi Chou, Yu-Han Chen, Yi-Ting Chen, Sung-Tsang Hsieh, Min-Fu Kuo, and Kuo-Ching Wang. Microcirculatory impairment and cerebral injury in hydrocephalus and the effects of cerebrospinal fluid diversion. *Neurosurgery*, 95(2):469–479, 2024.

Xiuyuan Liu, Giuseppe Barisano, Xiang Shao, Kay Jann, John M. Ringman, Hanzhang Lu, Kostas Arfanakis, Arvind Caprihan, Charles DeCarli, Brian T. Gold, Pauline Maillard, Claudia L. Satizabal, Ehsan Fadaee, Mohamied Habes, Laura Stables, Hardeep Singh, Bruce Fischl, Andre van der Kouwe, Karl Schwab, Kevin G. Helmer, Steven M. Greenberg, and David J. J. Wang. Cross-vendor test-retest validation of diffusion tensor image analysis along the perivascular space (dti-alps) for evaluating glymphatic system function. *Aging Dis*, 15(4):1885–1898, 2024. doi: 10.14336/AD.2023.0321-2.

Nanna MacAulay. Molecular mechanisms of brain water transport. *Nat Rev Neurosci*, 22: 326–344, 2021.

Gunnlaug Ringstad, Sarah A. S. Vatnehol, and Per K. Eide. Glymphatic mri in idiopathic normal pressure hydrocephalus. *Brain*, 140(10):2691–2705, 2017.

Toshiaki Taoka, Yasunari Masutani, Hiroki Kawai, Tomoyuki Nakane, Kentaro Matsuoka, Fumio Yasuno, Tatsuya Kishimoto, and Shinji Naganawa. Evaluation of glymphatic system activity with the diffusion mr technique: diffusion tensor image analysis along the perivascular space (dti-alps) in alzheimer's disease cases. *Jpn J Radiol*, 35(4):172–178, April 2017. doi: 10.1007/s11604-017-0617-z.

Toshiaki Taoka, Ryota Ito, Ryo Nakamichi, Tomoyuki Nakane, Hiroki Kawai, and Shinji Naganawa. Diffusion tensor image analysis along the perivascular space (dti-alps): Revisiting the meaning and significance of the method. *Magn Reson Med Sci*, 23(3):268–290, 2024. doi: 10.2463/mrms.rev.2023-0175.

Lu Zhou, Yanli Li, Erin M. Sweeney, X. H. Wang, Alexandra Kuceyeski, Gloria C. Chiang, Jana Ivanidze, Yi Wang, Stacy A. Gauthier, M. J. de Leon, and Thanh D. Nguyen. Association of brain tissue cerebrospinal fluid fraction with age in healthy cognitively normal adults. *Front Aging Neurosci*, 15:1162001, June 2023. doi: 10.3389/fnagi.2023.1162001.

David Ziegelitz, Jonas Arvidsson, Peter Hellström, Mai Tullberg, Carsten Wikkelsö, and Göran Starck. Pre-and postoperative cerebral blood flow changes in patients with idiopathic normal pressure hydrocephalus measured by computed tomography (ct)-perfusion. *Fluids Barriers CNS*, 12, 2015. Suppl 1:P59.